

## Insulating fcc $\text{YH}_{3-\delta}$ stabilized by $\text{MgH}_2$

S. J. van der Molen,\* D. G. Nagengast, A. T. M. van Gogh, J. Kalkman, E. S. Kooij, J. H. Rector, and R. Griessen  
*Faculty of Sciences, Division of Physics and Astronomy, Vrije Universiteit, De Boelelaan 1081, 1081 HV Amsterdam, The Netherlands*

(Received 5 December 2000; published 31 May 2001)

We study the structural, optical, and electrical properties of  $\text{Mg}_z\text{Y}_{1-z}$  switchable mirrors upon hydrogenation. It is found that the alloys disproportionate into essentially pure  $\text{YH}_{3-\delta}$  and  $\text{MgH}_2$  with the crystal structure of  $\text{YH}_{3-\delta}$  dependent on the Mg concentration  $z$ . For  $0 < z < 0.1$ , both hcp and fcc  $\text{YH}_{3-\delta}$  are observed, whereas for  $z \geq 0.1$  only cubic  $\text{YH}_{3-\delta}$  is present. Interestingly, cubic  $\text{YH}_{3-\delta}$  is expanded compared to  $\text{YH}_2$ , in disagreement with theoretical predictions. From optical and electrical measurements we conclude that cubic  $\text{YH}_{3-\delta}$  is a transparent insulator with properties similar to hexagonal  $\text{YH}_{3-\delta}$ . Our results are inconsistent with calculations predicting fcc  $\text{YH}_{3-\delta}$  to be metallic, but they are in good agreement with recent *GW* calculations on both hcp and fcc  $\text{YH}_3$ . Finally, we find an increase in the effective band gap of the hydrided  $\text{Mg}_z\text{Y}_{1-z}$  alloys with increasing  $z$ . Possibly this is due to quantum confinement effects in the small  $\text{YH}_3$  clusters.

DOI: 10.1103/PhysRevB.63.235116

PACS number(s): 73.61.-r, 68.60.-p, 78.66.-w

### I. INTRODUCTION

In 1996, Huiberts *et al.* reported that thin yttrium and lanthanum films exhibit spectacular changes in their optical properties upon hydrogenation.<sup>1-4</sup> The dihydrides are cubic metals that are reflective at energies lower than that of a characteristic transparency window (for  $\text{YH}_2$  at 1.8 eV); the trihydrides ( $\text{YH}_3$ , hexagonal;  $\text{LaH}_3$ , cubic) are transparent, large-gap semiconductors. Reversible switching between these two states is possible at ambient temperatures, by changing the surrounding hydrogen gas pressure<sup>1-4</sup> or electrolytic cell potential.<sup>5</sup> Besides  $\text{YH}_x$  and  $\text{LaH}_x$ , all trivalent rare earth hydrides ( $\text{RH}_x$ ) as well as their alloys with Mg exhibit similar switching properties,<sup>6-8</sup> hence the name ‘‘switchable mirrors’’ for the entire group. Switchable mirrors containing Mg are of special interest as they can be tailored to be reflective (i.e., the small transparency window is suppressed) and transparent over the entire optical range in the unloaded state and loaded state, respectively. Recently, it was shown that in these systems Mg acts as a microscopic, optical shutter,<sup>8</sup> changing from the shiny metal Mg to the large-gap insulator<sup>9,10</sup>  $\text{MgH}_2$  upon hydrogenation.

The insulating ground state of the rare earth trihydrides presented theorists with an interesting challenge. In the early 1990s, calculations on  $\text{YH}_3$  were performed in the local density approximation (LDA), using a variety of structures. However, in all cases, including the lowest energy hexagonal  $\text{HoD}_3$  structure, a metallic state was obtained.<sup>11,12</sup> The large discrepancy between experiment and LDA calculations stimulated other theorists to consider different approaches. Kelly *et al.*<sup>13</sup> demonstrate that small displacements of the hydrogen atoms, relative to the  $\text{HoD}_3$  structure, can induce a gap.<sup>14,15</sup> Ng *et al.*<sup>16</sup> and Eder *et al.*<sup>17</sup> on the other hand claim that strong electron correlation effects are the key ingredient in explaining the insulating state.<sup>18</sup>

The importance of electron correlation effects was also taken into account in *ab initio* band structure calculations using the *GW* approximation. van Gelderen *et al.*<sup>19</sup> performed calculations on  $\text{YH}_3$  in three hexagonal structures ( $\text{LaF}_3$ ,  $\text{HoD}_3$ , and the broken symmetry structure proposed

by Kelly *et al.*), whereas Miyake *et al.*<sup>20</sup> used the cubic  $\text{BiF}_3$  and hexagonal  $\text{LaF}_3$  structures. For the cubic as well as for the hexagonal cases,  $\text{YH}_3$  is found to be an insulator. These results are in disagreement with the work by Ahuja *et al.*<sup>21</sup> who claim that a hcp to fcc transition in  $\text{YH}_3$  is accompanied by an insulator to metal transition. Up to now, however, a comparison between cubic and hexagonal  $\text{YH}_3$  was not possible experimentally.

In this article we show that (i) one can stabilize fcc  $\text{YH}_3$  by alloying Y with Mg prior to hydrogenation; (ii) in contrast to  $\text{LaH}_x$ ,  $\text{YH}_x$  expands when loaded from dihydride to trihydride; (iii) fcc  $\text{YH}_{3-\delta}$  is a large-gap semiconductor similar to hcp  $\text{YH}_{3-\delta}$ ; (iv) the electrical properties of the hydrogenated alloys depend nontrivially on the Mg content.

### II. EXPERIMENT

A series of polycrystalline  $\text{Mg}_z\text{Y}_{1-z}$  samples of 300 nm thickness are prepared by coevaporation of Y and Mg under UHV conditions ( $10^{-9}$  mbar) on an *R*-plane  $\text{Al}_2\text{O}_3$  substrate using an electron gun and Knudsen cell, respectively. Two different geometries are used in this work. For the first, the complete  $\text{Mg}_z\text{Y}_{1-z}$  alloy is covered *in situ* with a 15 nm Pd layer. These samples are initially transferred to a Rigaku x-ray diffractometer and then to a Bruker IFS 66/S Fourier transform infrared spectrometer to study structural properties and optical transmission, respectively. The x-ray measurements are performed in a Bragg-Brentano geometry by moving the detector ( $2\Theta$ ) from  $10^\circ$  to  $75^\circ$  with a fixed sample angle of  $10^\circ$ . In both setups, hydrogenation (up to  $p_{\text{H}_2} = 1$  bar) is done slowly at room temperature, and checked by continuous recording of diffraction or optical transmission spectra. For the second set of samples, we use a geometry similar to the one introduced by den Broeder *et al.*<sup>3</sup> to study lateral H diffusion optically in switchable mirrors [see Fig. 4(a) below]. In this case, the  $\text{Mg}_z\text{Y}_{1-z}$  layer is only partly covered by Pd (making use of a shadow mask) after which the uncovered part of the alloy is superficially oxidized in ambient air. Subsequently, the sample is transferred either to the x-ray setup, or to a chamber equipped with

optical windows, temperature control, and electrical leads. This chamber is placed onto the positioning table of an optical microscope (Olympus BX60F5) on top of which a three-charge-coupled device camera is mounted. When 1 bar of  $H_2$  is introduced, the Pd covered part of the sample absorbs H immediately and switches to the fully hydrided state. However, hydrogen can enter the oxide covered  $Mg_z Y_{1-z}$  layer only by diffusing laterally out of the Pd covered area, as  $H_2$  dissociation is not possible at the oxide surface.<sup>22</sup> During the diffusion process, which can be followed optically, the hydride phases of the system are spatially separated. Phases with a high hydrogen concentration stay closest to the Pd strip.<sup>3,23</sup> A series of electrical contacts along the sample allows for resistivity measurements of the various areas. In this way, one circumvents electrical shortcut due to the Pd cap layer, which presents a problem for the first kind of sample. In this paper we mainly discuss the electric properties of the system. An extensive lateral diffusion study has also been performed but will not be reported on here.<sup>24</sup>

Sample composition (yielding the Mg content  $z$ ) and homogeneity are checked using Rutherford backscattering spectroscopy (RBS). The presence of a well-separated Pd peak shows that there is little interdiffusion of Pd and  $Mg_z Y_{1-z}$ . On one particular sample ( $Mg_{0.37}Y_{0.63}$ , second geometry), we performed scanning Auger microscopy (SAM) while the film was sputtered away. The resulting depth profile gives local chemical information.

### III. RESULTS AND DISCUSSION

#### A. Structure

First we focus on x-ray diffraction (XRD) analysis, starting with the virgin films. For  $0.01 \leq z \leq 0.37$ , XRD reveals the presence of two metallic phases, hcp  $\alpha$ -Y and cubic  $\gamma$ -YMg, which are randomly oriented. For  $z=0$  and  $z=0.5$ , we find only Y and YMg reflections, respectively. These results are in accordance with the Y-Mg phase diagram.<sup>25</sup> The absence of  $YMg_2$  peaks for  $z < 0.5$  confirms that our films are homogeneous in composition.

As soon as we load our samples with hydrogen,  $\gamma$ -YMg disproportionates into  $YH_2$  and Mg clusters,<sup>8</sup> an effect also found in other Mg alloys such as LaMg and CeMg.<sup>26,27</sup> Upon additional H uptake, small clusters of  $YH_{3-\delta}$  and  $MgH_2$  are formed. In Fig. 1, we show XRD spectra of a set of alloys in equilibrium with 1 bar  $H_2$  at room temperature. Note that only the  $YH_x$  peaks are observed due to the low Mg concentration and the large difference between the atomic form factors of Y and Mg (ratio 12:1). For comparison, peak positions of randomly oriented hcp  $YH_3$  and fcc  $YH_3$  (*a priori* assuming its existence) are indicated as well. The hcp reflections are calculated using bulk  $YH_3$  lattice constants<sup>28</sup> ( $a_0 = 0.3673$  nm and  $c_0 = 0.663$  nm). For an indication of the fcc peak positions, we initially assume that fcc and hcp  $YH_3$  have equal volume per formula unit, implying a fcc lattice constant  $a_{fcc} = 0.537$  nm. Inspecting Fig. 1 for Mg concentrations  $z=0.01$  and  $z=0.03$ , we find that  $YH_{3-\delta}$  is present in both cubic and hexagonal symmetry, with peak positions at  $29^\circ$  [fcc (111)] and  $34^\circ$  [fcc (200)], as well as at  $27^\circ$  [hcp

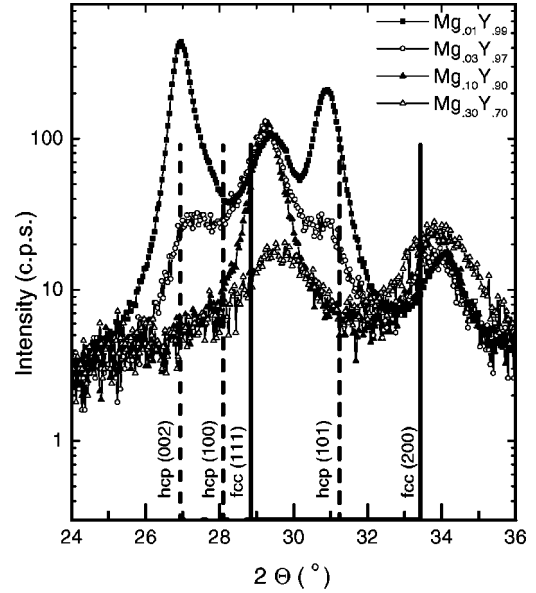


FIG. 1. X-ray diffraction measurements in Bragg-Brentano geometry ( $\Theta = 10^\circ$ ) of  $Mg_z Y_{1-z}$  films after hydrogenation in 1 bar  $H_2$  at room temperature. For clarity, only four results are shown ( $z = 0.01, 0.03, 0.10$ , and  $0.30$ ), in a limited  $2\Theta$  range. Furthermore, the diffraction lines of hcp  $YH_3$  (dashed) and hypothetical fcc  $YH_3$  (solid) are displayed, the latter lines having been calculated assuming  $V_{YH_3}^{fcc} = V_{YH_3}^{hcp}$ . Comparing our data with these lines, we conclude that a transition from hcp  $YH_3$  (at  $z=0$ ) to fcc  $YH_3$  (at  $z=0.10$ ) takes place with increasing  $z$ .

(002)] and  $31^\circ$  [hcp (101)]. For Mg concentrations  $z \geq 0.10$ , however, only fcc  $YH_{3-\delta}$  is observed.

Figure 2 shows the volume per  $YH_{3-\delta}$  formula unit as a function of Mg concentration in the fully hydrided alloys.<sup>29</sup> In the fcc-hcp coexistence region ( $z < 0.10$ ), the unit cell volume of both structural phases is approximately independent of  $z$ . However, for  $z \geq 0.10$ , where hcp  $YH_{3-\delta}$  is no longer present, the unit cell volume of fcc  $YH_{3-\delta}$  decreases with increasing Mg content. Both these phenomena can be understood by considering the volume expansions of Y and Mg during hydrogenation.<sup>30</sup> Upon transforming to hcp  $YH_{3-\delta}$ , bulk Y expands by approximately 17%, mostly in the out-of-plane direction.<sup>28</sup> The transition from Mg to  $MgH_2$ , however, involves a volume increase of as much as 32%.<sup>10,31</sup> This enormous expansion causes large stresses in the film.<sup>8,32</sup> For  $z < 0.10$ , the system is able to reduce the internal pressure by transforming hcp  $YH_{3-\delta}$  to the smaller fcc  $YH_{3-\delta}$ . For  $z \geq 0.10$ , this is no longer possible and the fcc  $YH_{3-\delta}$  is increasingly compressed with increasing Mg content.

A transition from hcp to fcc  $YH_{3-\delta}$  was indeed predicted by Ahuja *et al.*<sup>21,33</sup> However, there is a large difference between the theoretically calculated and the experimentally observed volumes per formula unit. Whereas Ahuja *et al.* expect  $36.4 \text{ \AA}^3$  for hcp  $YH_{3-\delta}$  and  $32.3 \text{ \AA}^3$  for fcc  $YH_{3-\delta}$ , we find  $V_{hcp}(z < 0.1) = 39.5 \text{ \AA}^3$  and  $V_{fcc}(z < 0.1) = 36.9 \text{ \AA}^3$ .

Figure 2 also shows the volume of fcc  $YH_2$  as determined after unloading the films. Once more, we observe a plateau for  $z < 0.10$  (where the dihydride volume has the bulk value<sup>28</sup>

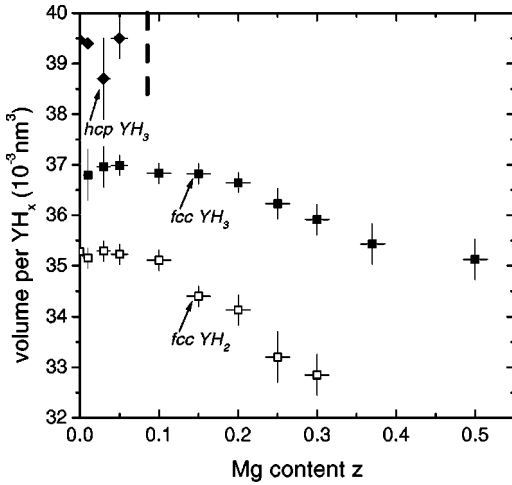


FIG. 2. Closed symbols: Volume of  $\text{YH}_3$  (per formula unit) in fully hydrogenated  $\text{Mg}_z\text{Y}_{1-z}$  alloys as a function of  $z$  ( $p_{\text{H}_2} = 1$  bar, room temperature). For  $z \leq 0.1$ , there is a two-phase region of hcp  $\text{YH}_3$  (diamonds) and fcc  $\text{YH}_3$  (solid squares). For  $z \geq 0.1$  only fcc  $\text{YH}_3$  is present. Open symbols: Volume of  $\text{YH}_2$  (per formula unit) as measured after unloading the samples.

$35.2 \text{ \AA}^3$ ) and a decrease for  $z > 0.1$ . Interestingly, the volume change upon loading from  $\text{YH}_{2-\varepsilon}$  to  $\text{YH}_{3-\delta}$  is positive for all  $z$ . At first glance, this is a rather surprising result. It is well known that fcc  $\text{LaH}_2$  contracts upon loading to fcc  $\text{LaH}_3$ . Furthermore, calculations by Sun *et al.* predict that fcc  $\text{YH}_3$  has a smaller volume than fcc  $\text{YH}_2$  ( $34.5 \text{ \AA}^3$  and  $35.1 \text{ \AA}^3$  per formula unit, respectively).<sup>34</sup> However, our results are consistent with the recent work by van Gogh *et al.*<sup>35</sup> who performed a study of the  $\text{La}_{1-y}\text{Y}_y\text{H}_x$  system. In contrast to the films studied here, their samples show no segregation upon hydrogen loading, i.e., Y and La stay mixed on an atomic scale. van Gogh *et al.* find that (i)  $\text{La}_{1-y}\text{Y}_y\text{H}_3$  is cubic for  $y < 0.67$  and (ii)  $\text{La}_{1-y}\text{Y}_y\text{H}_x$  contracts for  $y < 0.38$ , but expands for  $y > 0.38$ , when  $x$  increases from 2 to 3. These results suggest strongly that if fcc  $\text{YH}_3$  exists its volume should be larger than that of fcc  $\text{YH}_2$ . Extrapolating the volumes of the fcc trihydrides  $\text{La}_{1-y}\text{Y}_y\text{H}_3$  to  $y = 1$  (i.e., to ‘‘pure fcc  $\text{YH}_3$ ’’) one obtains a value of  $38 \text{ \AA}^3$ . This is somewhat larger than the fcc  $\text{YH}_3$  volumes in Fig. 2, a difference that may be attributed to the different way the Y is distributed in the two systems (mixing on an atomic scale versus segregation) as well as to the different stress states.

### B. Optical transmission

In the inset of Fig. 3, the optical transmittance  $T_{opt}$  as a function of photon energy is shown for three alloys ( $z = 0.01, 0.15, 0.30$ ) in equilibrium with 1 bar  $\text{H}_2$  at room temperature. Clearly, the addition of Mg makes these switchable mirrors more transparent and more color neutral in the loaded state. From the optical transmission curves we determine an effective optical gap  $E_{gap}^{opt}$  defined arbitrarily as the energy at which  $T_{opt}$  falls below 0.3%. The main frame of Fig. 3 shows this quantity as a function of  $z$ .

Let us first focus on the two-phase fcc-hcp  $\text{YH}_3$  region ( $z < 0.1$ ). In this interval, the optical gap does not change

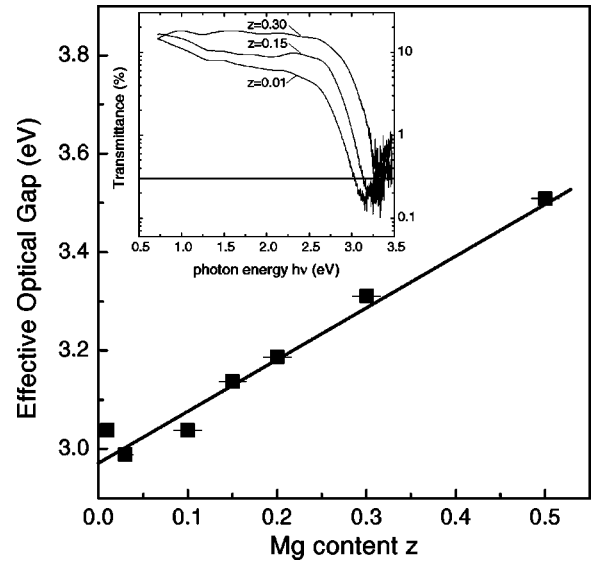


FIG. 3. Effective optical band gap  $E_{gap}^{opt}$  versus Mg content  $z$ . The inset shows the optical transmittance  $T_{opt}$  as a function of photon energy  $h\nu$  for three hydrogenated films ( $z = 0.01, 0.15$ , and  $0.30$ ). The effective optical gap  $E_{gap}^{opt}$  is defined here as the energy at which  $T_{opt}$  drops below 0.3%. The line is a guide to the eye.

significantly with  $z$ , although hcp  $\text{YH}_3$  is increasingly substituted by fcc  $\text{YH}_3$ . Since  $\text{MgH}_2$  is a large-gap insulator (a very recent measurement<sup>9</sup> yields an optical gap of approximately 6 eV), this is only possible if the optical properties of fcc  $\text{YH}_3$  are comparable to those of hcp  $\text{YH}_3$ . Therefore, the optical measurements suggest strongly that fcc  $\text{YH}_3$  is a large-gap semiconductor just like hcp  $\text{YH}_3$ . This conclusion is substantiated by the electrical resistivity data presented in Sec. III C.

Next, we focus on the region  $z \geq 0.10$  where only fcc  $\text{YH}_3$  and  $\text{MgH}_2$  are present. Figure 3 shows that the optical band gap increases nearly linearly with  $z$ , i.e., when  $\text{YH}_3$  is gradually replaced by  $\text{MgH}_2$ . To obtain an intuitive picture of this effect, we first consider the simplest possible model. The cluster size of  $\text{YH}_3$  being much smaller than the film thickness (see below), a simple optical analogy is a double layer structure of  $\text{YH}_3$  [with layer thickness  $d_{\text{YH}_3}(z)$ ] and  $\text{MgH}_2$ . As the optical gap of  $\text{MgH}_2$  is much larger than that of  $\text{YH}_3$ , (i.e.,  $\text{MgH}_2$  is basically transparent in the energy range of our measurements),  $T_{opt}$  is dominated by  $\text{YH}_3$ . For a double layer, we approximately have the Lambert-Beer relation  $T_{opt}(h\nu) \approx T_0 \exp[-\alpha_{\text{YH}_3}(h\nu)d_{\text{YH}_3}]$ , where  $T_0$  and  $\alpha_{\text{YH}_3}(h\nu)$  denote the original light intensity and the energy dependent absorption coefficient of  $\text{YH}_3$ , respectively. Since  $d_{\text{YH}_3}(z) \propto (1-z)$ , this relation predicts an exponentially increasing transmission over the entire energy range with increasing  $z$ . As a consequence of its definition, this implies a higher effective optical gap. Figure 3 shows that both these effects do indeed occur in the alloys.

Interestingly though, the two-layer model fails to work on closer inspection. This is seen in the work by Giebels *et al.*<sup>36</sup> who compare the optical properties of hydrogenated  $\text{Mg}_z\text{Y}_{1-z}$  alloys with those of multilayers with equal overall

composition. They find that the effective optical gap of an alloy shifts to higher energies than that of a multilayer. In other words, a quantitative description of the optics of loaded  $\text{Mg}_z\text{Y}_{1-z}$  alloys is not possible just using a layered model. A reason for this may be that the  $\text{MgH}_2$  clusters have an irregular distribution through the film (unfortunately the x-ray data do not allow for a  $\text{MgH}_2$  cluster size determination for low  $z$ ). Another, much more fundamental, cause could be a mutual influence of  $\text{MgH}_2$  and  $\text{YH}_3$  clusters, perhaps of electronic origin. This is discussed in Sec. III C.

Finally, we report on an interesting consequence of the suppression of the fcc  $\text{YH}_2$  to hcp  $\text{YH}_3$  structural phase transition: there is a large increase in the size of the thermochromic effect<sup>24,37</sup> for samples in which fcc  $\text{YH}_3$  instead of hcp  $\text{YH}_3$  is formed (i.e., for  $z \geq 0.1$ ). Most likely, this is due to a difference between the fcc- $\text{YH}_2$ /hcp- $\text{YH}_3$  isotherms and the fcc- $\text{YH}_2$ /fcc- $\text{YH}_3$  isotherms, the latter probably being less steep near  $x=3$ . As a result, the equilibrium H concentration (and therefore the optical transmission) in 1 bar  $\text{H}_2$  is much more temperature dependent for fcc  $\text{YH}_{3-\delta}$  than for hcp  $\text{YH}_{3-\delta}$ .

### C. Resistivity

To confirm the insulating nature of the hydrided samples, a series of resistivity measurements are performed. Unfortunately, it is difficult to accurately determine the resistivity of the transparent layer for the first kind of sample. This is due to the 15 nm Pd cap layer shunting the insulating layer. To circumvent this problem, we use samples of the second geometry [see Fig. 4(a)]. As explained above, a lateral diffusion process takes place in these samples,<sup>3,23</sup> as soon as they are in contact with 1 bar  $\text{H}_2$ . During the process, the transparent phase appears next to the Pd cap layer, slowly growing away from the Pd edges. To accelerate its migration, we apply a voltage to the sample. As a result, the transparent phase grows in the direction of the anode with constant velocity.<sup>38</sup> This implies that H in the insulating phase behaves as a negative particle, consistent with our recent work<sup>18,38,39</sup> on  $\text{YH}_{3-\delta}$ .

When the insulating phase has moved by more than  $100 \mu\text{m}$  from the Pd edge [see Fig. 4(b)], we determine its resistance. Figure 4(c) shows the room temperature resistivity  $\rho$  of the insulating area in the diffusion samples as a function of Mg content  $z$ . A remarkable relation is observed:  $\rho$  grows almost exponentially with  $z$ , increasing by as much as four orders of magnitude from  $z=0$  to  $z=0.25$ . The data point at  $z=0.37$  deviates from the general trend. We note, however, that on this sample a dense pattern of hillocks appeared at the oxide surface [see inset Fig. 4(c)]. SAM depth profiles taken at and away from two hillocks yield a large variation in Mg content. Hillocks turn out to be Mg rich, whereas the rest of the film is Mg poor. Therefore, the data point initially at  $z=0.37$  should probably be shifted toward the left in Fig. 4(c). The profiles taken away from the hillocks show a nearly constant Mg content as a function of depth, once more confirming the homogeneity of the as-deposited films.

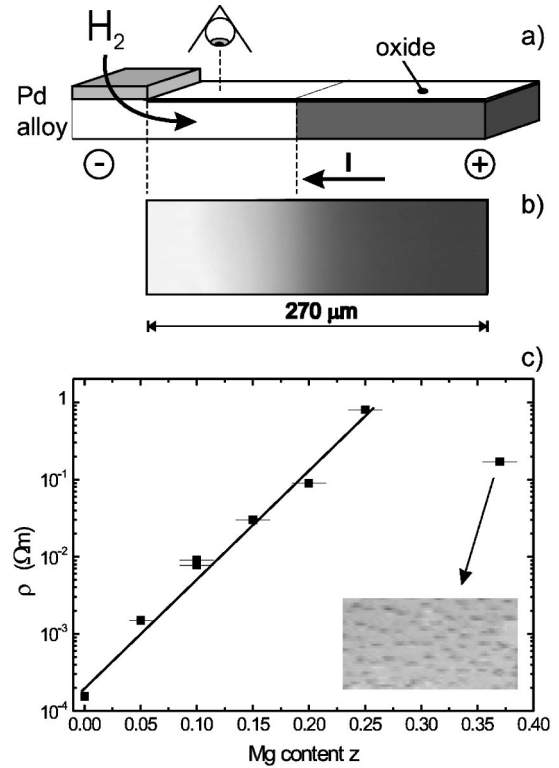


FIG. 4. (a) Geometry of a lateral diffusion sample. In 1 bar  $\text{H}_2$ , hydrogen enters the film via the Pd strip and migrates laterally underneath the superficial oxide layer. Upon applying a current through the sample, the transparent hydride phase is attracted by the (+) pole. (b) Micrograph in optical transmission of one of the  $\text{Mg}_{0.10}\text{Y}_{0.90}$  samples after lateral H migration. For clarity, the Pd covered area is not shown. When the transparent area has grown large enough, its resistance is measured. (c) Resistivity  $\rho$  of the transparent area versus Mg content  $z$ . The line is a guide to the eye. Shown in the inset is a transmission picture [same scale as (b)] of the  $\text{Mg}_{0.37}\text{Y}_{0.63}$  sample, on which a dense hillock pattern is observed.

The main message of Fig. 4(c) is that the resistivity of fcc  $\text{YH}_{3-\delta}$  is equal to or larger than that of hcp  $\text{YH}_{3-\delta}$ . If this were not the case, the sample resistivity would drop from  $z=0$  to  $z=0.10$ , i.e., when hcp  $\text{YH}_3$  is substituted by fcc  $\text{YH}_3$ . We note that at such low  $\text{MgH}_2$  content no serious percolation problems are expected (as argued below). From the combination of optical transmission and electrical transport data, we conclude that fcc  $\text{YH}_{3-\delta}$  is an insulator with a gap comparable to (if not larger than) that of hcp  $\text{YH}_{3-\delta}$ . This result is in flagrant disagreement with the prediction by Ahuja *et al.*<sup>21</sup> that a transition from hcp to fcc  $\text{YH}_3$  is accompanied by an insulator-metal transition. Moreover, it shows that the insulating nature of  $\text{YH}_3$  is not very sensitive to its precise lattice structure at all; the dominant parameter determining the electronic state of  $\text{YH}_x$  seems to be the hydrogen concentration. This suggests that the band gap is primarily controlled by the electronic interactions in the system.<sup>20</sup> Interestingly, these conclusions are consistent with recent *GW* calculations, which show that  $\text{YH}_3$  is insulating in four quite different structures.<sup>19,20</sup> Our results are also in agreement with the strong correlation theories proposed by Ng *et al.*

and Eder *et al.* as these are inherently of local character.<sup>16,17</sup> Unfortunately, we are not aware of calculations on various structures using either of the latter models.

Finally, it seems that the insensitivity of the insulating state to structural changes is not in agreement with the original calculations by Kelly *et al.*<sup>13</sup> In their view, subtle rearrangements of the (hydrogen) lattice are responsible for the insulating ground state. Without these,  $\text{YH}_3$  would be metallic. We do note, though, that the recent calculations by van Gelderen *et al.*<sup>19</sup> do not show much difference between the  $\text{HoD}_3$  and the broken symmetry structures: both have a comparable gap in the  $GW$  approximation. Thus, although the broken symmetry structure may exist,<sup>40</sup> its presence is not a prerequisite for an insulating ground state.

Figure 4(c) not only confirms the insulating nature of fcc  $\text{YH}_3$ , it also shows an almost exponential dependence of the film resistivity on Mg content. In the following, we discuss a number of explanations for this relation, starting with two trivial ones. A first possibility is that the films have oxidized heavily, resulting in a large increase of resistivity. This hypothesis is easily rejected, since both RBS and SAM depth profiles show that the lowest 60% of the films is oxygen-free (see also Ref. 22). Furthermore, we tested reversibility by unloading the films in air, pushing the insulating area back to the Pd by the use of a (positive) voltage.<sup>3</sup> After unloading, the resistivity of the oxide covered part of the films is approximately equal to that of the virgin films ( $\sim 10^{-6}\Omega \text{ m}$ ), i.e., many orders of magnitude smaller than in the hydrided state. Since oxidation of switchable mirrors is irreversible, this experiment tells us that the results in Fig. 4(c) are entirely due to hydrogenation.

Next, we focus on the composition of the insulating area. As mentioned above, disproportionation leads to the formation of clusters of  $\text{YH}_{3-\delta}$  (possibly doped with Mg), as well as clusters of  $\text{MgH}_2$ . The resistivity of pure  $\text{YH}_{3-\delta}$  is known to be relatively low ( $\sim 10^{-4}\Omega \text{ m}$  in 1 bar  $\text{H}_2$ ), despite its large optical band gap. This is due to the fact that H vacancies in  $\text{YH}_{3-\delta}$  act as donors,<sup>41,42</sup> and thereby determine the conductivity, i.e.,  $\rho = 1/\sigma \propto 1/\delta$  in  $\text{YH}_{3-\delta}$ . On the other hand,  $\text{MgH}_2$  is an insulator with a gap of approximately 6 eV and a resistivity much higher than  $\text{YH}_{3-\delta}$ . The large conductivity difference between the two cluster species suggests that Fig. 4(c) may well be the result of a classical percolation problem: with increasing number of  $\text{MgH}_2$  clusters, fewer and fewer current paths through the  $\text{YH}_{3-\delta}$  are available, resulting in a drastic resistivity increase near the percolation threshold (where no such path exists). Comparison with percolation theory, however,<sup>43</sup> immediately shows that this cannot be the main mechanism here. Percolation thresholds lie around 75 (50) vol % of low conductivity material for three (two) dimensions, whereas here we already see a large effect when only a few volume percent of  $\text{MgH}_2$  is present. (Note that  $z=0.25$  corresponds to 23 vol % of  $\text{MgH}_2$ .) Furthermore, Fig. 4(c) does not exhibit power law behavior.<sup>43</sup> Having rejected oxidation and percolation as explanations, we conclude that the resistivity measured in our films is dominated by the  $\text{YH}_{3-\delta}$  clusters, and not by  $\text{MgH}_2$ , or any oxide.

The rest of this section will therefore focus on the question of how the properties of the  $\text{YH}_{3-\delta}$  clusters are influenced by the presence of Mg. Let us consider the possibility that  $\text{YH}_{3-\delta}$  clusters themselves contain Mg impurities (i.e., on an atomic scale, apart from the clusters of  $\text{MgH}_2$ ). Since Mg has only two valence electrons whereas Y has three, a Mg atom in an  $\text{YH}_{3-\delta}$  matrix may act as an acceptor, compensating for the electrons donated by H vacancies. Consequently, the resistance of  $\text{YH}_{3-\delta}$  clusters increases with increasing concentration of Mg impurities, i.e., with increasing  $z$ . This leads to the expectation  $\rho(z) \propto [n(\delta, z=0) - N_{\text{Mg}}(z)]^{-1}$ , where  $n(\delta, z=0)$  is the electron density in  $\text{YH}_{3-\delta}$  and  $N_{\text{Mg}}(z)$  is the concentration of Mg impurities in the  $\text{YH}_{3-\delta}$  grains. Although this effect goes in the right direction, it is clear that it cannot explain the exponential behavior of Fig. 4(c). Moreover, exponential resistivity behavior is in general expected only if there is a change in some energy parameter. Therefore, we consider the effects of a change in the  $\text{YH}_3$  heat of formation  $\Delta H$  as a function of  $z$ . For a metal-hydride system in equilibrium with  $\text{H}_2$ , the hydrogen concentration is directly related to  $\Delta H$ : the more negative  $\Delta H$ , the larger the concentration and, consequently, the lower the H vacancy concentration and the higher the resistivity. Suppose  $\Delta H$  depends on  $z$  via  $\Delta H(z) = \Delta H_0 - \alpha z$  where  $\Delta H_0$  is the enthalpy of formation of Mg-free  $\text{YH}_{3-\delta}$ . For an  $\text{YH}_{3-\delta}$  sample in equilibrium with  $\text{H}_2$  gas at chemical potential  $\mu_{\text{H}_2}$ , the lattice gas model of Lacher<sup>44</sup> yields

$$\frac{1}{2}RT \ln\left(\frac{p_{\text{H}_2}}{p_0(T)}\right) = RT \ln\left(\frac{1-\delta(z)}{\delta(z)}\right) + \Delta H_0 - \alpha z, \quad (1)$$

where  $p_0(T) \propto T^{7/2}$  is a reference pressure and  $R$  is the gas constant. Solving for  $\delta(z)$ , we find

$$\begin{aligned} \delta(z) &= \left[ 1 + \sqrt{\frac{p_{\text{H}_2}}{p_0(T)} \exp\left(\frac{-\Delta H_0 + \alpha z}{RT}\right)} \right]^{-1} \\ &\approx \sqrt{\frac{p_0(T)}{p_{\text{H}_2}}} \exp\left(\frac{\Delta H_0 - \alpha z}{RT}\right) \equiv \delta(z=0) \exp\left(\frac{-\alpha z}{RT}\right). \end{aligned} \quad (2)$$

Hence, since  $\rho \propto 1/\delta$ ,

$$\rho(z) \approx \rho(z=0) \exp\left(\frac{\alpha z}{RT}\right), \quad (3)$$

where  $\rho(z=0)$  represents the resistivity of Mg-free  $\text{YH}_{3-\delta}$ . Clearly, this gives a form compatible with Fig. 4(c) if  $\alpha > 0$ , i.e., if  $\Delta H$  decreases with increasing  $z$ . Electrochemical measurements, however, show that this is not at all the case:<sup>36</sup>  $\Delta H$  increases (toward zero) with increasing  $z$ . This is confirmed by a crude estimation of the change  $d\Delta H$  due to stress in the films. For this we make use of the relation  $d\Delta H = -BV_{\text{H}}dV/V$  (see Ref. 8), where  $B$  is the  $\text{YH}_3$  bulk modulus,  $V_{\text{H}}$  is the volume change upon addition of 1 mole of hydrogen, and  $dV$  is the volume change due to stress. From Fig. 2 we have  $V_{\text{H}} > 0$  (the volume increases upon

hydrogen uptake) as well as  $V(z) \leq V(z=0)$  and thus  $dV \leq 0$  (the volume decreases upon Mg addition, as a result of stress). This yields  $d\Delta H(z) > 0$ . Consequently, the resistivity change in Fig. 4(c) is not due to a change in  $\Delta H$ .

Since the foregoing mostly nonelectronic pictures fail, we finally discuss the possibility that the band structure of  $\text{YH}_{3-\delta}$  is influenced by the presence of  $\text{MgH}_2$ . In fact, one way to interpret the optical data of Fig. 3 and the differences between alloys and multilayers is that the band gap of  $\text{YH}_{3-\delta}$  increases with increasing  $z$ . Interestingly, such an effect could also explain the resistivity data. If we assume the simple relation  $\rho(z) = \rho(z=0) \exp[E_{\text{gap}}^p(z)/2k_B T]$  and calculate  $E_{\text{gap}}^p$  as a function of  $z$  from Fig. 4(c), we find that  $\Delta E_{\text{gap}}^p / \Delta z = 1.6$  eV. This is close to the change in the effective optical gap obtained from Fig. 3,  $\Delta E_{\text{gap}}^{\text{opt}} / \Delta z = 1.1$  eV, indicating that the same physical phenomenon lies at the heart of both Figs. 3 and 4(c). We discuss two possible reasons for a shift of electron energy levels: band bending and quantum confinement. Both are related to the small size of the  $\text{YH}_3$  clusters.

The first effect occurs when the bands of  $\text{YH}_3$  bend in the contact region with  $\text{MgH}_2$  (compare, e.g., GaAs- $\text{Al}_x\text{Ga}_{1-x}\text{As}$  nanostructures). If the spatial extent of band bending is comparable to the  $\text{YH}_3$  cluster size, the effective band gap of  $\text{YH}_3$  increases, because the ‘‘bulk’’ gap value is not reached within the cluster. We note, however, that due to the low carrier concentration in  $\text{MgH}_2$  one does not expect band bending to be of key importance.

Quantum confinement has been put forward to explain cluster size dependent luminescence in nanocrystalline or porous Si.<sup>45,46</sup> The smaller a cluster, the higher the energy levels, as in the textbook particle-in-a-box problem. A reasonable estimate is<sup>45</sup>

$$\Delta E_{\text{gap}}^{\text{QC}}(L) \approx \frac{2\pi^2 \hbar^2}{L^2} \left( \frac{1}{m_e^*} + \frac{1}{m_h^*} \right), \quad (4)$$

where  $m_{e(h)}^*$  denotes the electron (hole) effective mass and  $L$  is the diameter of the  $\text{YH}_3$  clusters. To estimate  $L$ , we use the x-ray coherence length  $l_{\text{coh}}$ , which is determined from the width of the XRD peaks via the Debye-Scherrer formula. As seen in Fig. 5(a),  $l_{\text{coh}}$  decreases as a function of Mg content  $z$ , from  $l_{\text{coh}} = 18$  nm for  $z=0$  to  $l_{\text{coh}} = 4$  nm for  $z=0.3$ . To calculate the energy shift due to quantum confinement, we need the effective masses  $m_e^*$  and  $m_h^*$  in  $\text{YH}_3$ . Since no experimental data are available, we use the *GW* band structure calculations by van Gelderen *et al.*<sup>19</sup> to obtain  $m_e^* \approx 0.35m_e$  and  $m_h^* \approx -0.74m_e$ . In Fig. 5(b), we plot  $\Delta E_{\text{gap}}^{\text{QC}}$  as a function of  $z$ , calculated using Eq. (4) and presuming that  $L = l_{\text{coh}}$ . As  $z$  increases,  $\Delta E_{\text{gap}}^{\text{QC}}$  increases significantly, and we have approximately  $\Delta E_{\text{gap}}^{\text{QC}} / \Delta z \approx 0.3$  eV/0.3 = 1 eV. This change is remarkably close to the increase observed in Figs. 3 and 4(c). Therefore, it is conceivable that quantum confinement effects play an important role in hydrided  $\text{Mg}_z\text{Y}_{1-z}$  alloys.

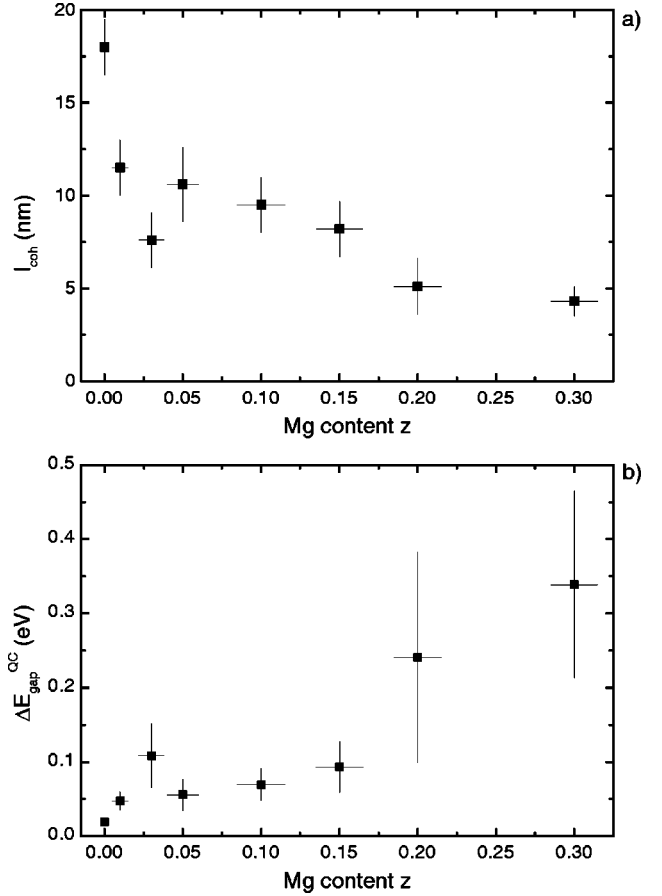


FIG. 5. (a) X-ray coherence length  $l_{\text{coh}}$  of the  $\text{YH}_3$  clusters in fully hydrogenated  $\text{Mg}_z\text{Y}_{1-z}$  alloys versus  $z$ . (b) Change in band gap  $\Delta E_{\text{gap}}^{\text{QC}}(z)$  as a result of quantum confinement. To estimate  $\Delta E_{\text{gap}}^{\text{QC}}$ , we use Eq. (4) and assume  $L = l_{\text{coh}}$ .

#### IV. CONCLUSIONS

We have synthesized fcc  $\text{YH}_{3-\delta}$  making use of the disproportionation reaction and stresses in  $\text{Mg}_z\text{Y}_{1-z}$  films upon hydrogen loading. In contrast to  $\text{LaH}_x$  as well as to theoretical predictions, fcc  $\text{YH}_3$  has a larger unit cell volume than fcc  $\text{YH}_2$ . Furthermore, it is an insulator with a gap comparable to that of hcp  $\text{YH}_{3-\delta}$ , as concluded from optical transmittance and resistivity measurements. This result is in clear disagreement with the prediction by Ahuja *et al.* that fcc  $\text{YH}_{3-\delta}$  should be metallic. The fact that the properties of  $\text{YH}_{3-\delta}$  are not at all sensitive to the exact crystal structure is consistent with a series of recent *GW* calculations. Furthermore, it is compatible with the essentially local models proposed by Ng *et al.* and by Eder *et al.*

There is a rather large influence of the Mg content on the overall film properties. The effective optical gap, defined here as the energy at which the transmittance is 0.3%, increases linearly with  $z$ . Furthermore, the sample resistivity (as measured in a lateral diffusion geometry) increases exponentially with  $z$ . Although the optical data alone could have a trivial explanation (the cluster distribution is essential in optics), the combination of both data sets hints at a change in the  $\text{YH}_{3-\delta}$  band structure as a function of  $z$ . Possibly, this is

a result of quantum confinement effects in the small  $\text{YH}_3$  clusters.

#### ACKNOWLEDGMENTS

The authors acknowledge useful discussions with P. van der Sluis, A. Remhof, and I. A. M. E. Giebels and thank N.

J. Koeman for technical support. This work is part of the research program of the Dutch Stichting voor Fundamenteel Onderzoek der Materie (FOM) which is financially supported by NWO, and of the TMR Research Network ‘‘Switchable Metal-Hydride Films.’’

\*Electronic address: sejan@nat.vu.nl

- <sup>1</sup>J.N. Huiberts, R. Griessen, J.H. Rector, R.J. Wijngaarden, J.P. Dekker, D.G. de Groot, and N.J. Koeman, *Nature (London)* **380**, 231 (1996).
- <sup>2</sup>J.N. Huiberts, J.H. Rector, R.J. Wijngaarden, S. Jetten, D. de Groot, B. Dam, N.J. Koeman, R. Griessen, B. Hjörvarsson, S. Olafson, and Y.S. Cho, *J. Alloys Compd.* **239**, 158 (1996).
- <sup>3</sup>F.J.A. den Broeder, S.J. van der Molen, M. Kremers, J.N. Huiberts, D.G. Nagengast, A.T.M. van Gogh, M. Huisman, N.J. Koeman, B. Dam, J.H. Rector, S. Plota, M. Haaksma, R.M. Jungblut, P.A. Duine, and R. Griessen, *Nature (London)* **394**, 656 (1998).
- <sup>4</sup>J.W.J. Kerssemakers, S.J. van der Molen, N.J. Koeman, R. Günther, and R. Griessen, *Nature (London)* **406**, 489 (2000).
- <sup>5</sup>P.H.L. Notten, M. Kremers, and R. Griessen, *J. Electrochem. Soc.* **143**, 3348 (1996); M. Kremers, N.J. Koeman, R. Griessen, P.H.L. Notten, R. Tolboom, P.J. Kelly, and P.A. Duine, *Phys. Rev. B* **57**, 4943 (1998); E.S. Kooij, A.T.M. van Gogh, and R. Griessen, *J. Electrochem. Soc.* **146**, 2990 (1999); E.S. Kooij, A.T.M. van Gogh, D.G. Nagengast, N.J. Koeman, and R. Griessen, *Phys. Rev. B* **62**, 10 088 (2000).
- <sup>6</sup>P. van der Sluis, M. Ouwkerk, and P.A. Duine, *Appl. Phys. Lett.* **70**, 3356 (1997); R. Armitage, M. Rubin, T. Richardson, N. O’Brien, and Yong Chen, *ibid.* **75**, 1863 (1999).
- <sup>7</sup>P. van der Sluis, *Appl. Phys. Lett.* **73**, 1826 (1998).
- <sup>8</sup>D.G. Nagengast, A.T.M. van Gogh, E.S. Kooij, B. Dam, and R. Griessen, *Appl. Phys. Lett.* **75**, 2050 (1999).
- <sup>9</sup>K. Yamamoto, K. Higuchi, H. Kajioka, H. Sumida, S. Orimo, and H. Fujii (unpublished).
- <sup>10</sup>R. Yu and P.K. Lam, *Phys. Rev. B* **37**, 8730 (1988); I. Baraille, C. Pouchan, M. Causa, and C. Pisani, *Chem. Phys.* **179**, 39 (1994).
- <sup>11</sup>X. Wang and M.Y. Chou, *Phys. Rev. Lett.* **71**, 1226 (1993); *Phys. Rev. B* **51**, 7500 (1995).
- <sup>12</sup>J.P. Dekker, J. van Ek, A. Lodder, and J.N. Huiberts, *J. Phys.: Condens. Matter* **54**, 48 055 (1993).
- <sup>13</sup>P.J. Kelly, J.P. Dekker, and R. Stumpf, *Phys. Rev. Lett.* **78**, 1315 (1997).
- <sup>14</sup>T.J. Udovic, Q. Huang, and J.J. Rush, *Phys. Rev. Lett.* **79**, 2920 (1997); P.J. Kelly, J.P. Dekker, and R. Stumpf, *ibid.* **79**, 2921 (1997).
- <sup>15</sup>A.T.M. van Gogh, E.S. Kooij, and R. Griessen, *Phys. Rev. Lett.* **83**, 4614 (1999).
- <sup>16</sup>K.K. Ng, F.C. Zhang, V.I. Anisimov, and T.M. Rice, *Phys. Rev. Lett.* **78**, 1311 (1997); *Phys. Rev. B* **59**, 5398 (1999).
- <sup>17</sup>R. Eder, H.F. Pen, and G.A. Sawatzky, *Phys. Rev. B* **56**, 10 115 (1997).
- <sup>18</sup>S.J. van der Molen, M.S. Welling, and R. Griessen, *Phys. Rev. Lett.* **85**, 3882 (2000).
- <sup>19</sup>P. van Gelderen, P.A. Bobbert, P.J. Kelly, and G. Brocks, *Phys. Rev. Lett.* **85**, 2989 (2000).
- <sup>20</sup>T. Miyake, R. Aryasetiawan, H. Kino, and K. Terakura, *Phys. Rev. B* **61**, 16 491 (2000).
- <sup>21</sup>R. Ahuja, B. Johansson, J.M. Willis, and O. Eriksson, *Appl. Phys. Lett.* **71**, 3498 (1997).
- <sup>22</sup>S.J. van der Molen, J.W.J. Kerssemakers, J.H. Rector, N.J. Koeman, B. Dam, and R. Griessen, *J. Appl. Phys.* **86**, 6107 (1999).
- <sup>23</sup>M.C. Huisman, S.J. van der Molen, and R.D. Vis, *Nucl. Instrum. Methods Phys. Res. B* **158**, 451 (1999); A. Remhof, G. Song, C. Sutter, D. Labergerie, M. Hübener, H. Zabel, and J. Härtwig, *Phys. Rev. B* **62**, 2164 (2000).
- <sup>24</sup>S. J. van der Molen, Ph.D. thesis, Vrije Universiteit, Amsterdam, The Netherlands, 2001.
- <sup>25</sup>J.F. Smith, D.M. Bailey, D.B. Novotny, and J.E. Davison, *Acta Metall.* **13**, 889 (1965).
- <sup>26</sup>M. Pezat, B. Darriet, and P. Hagenmuller, *J. Less-Common Met.* **74**, 427 (1980); J. Isidorsson, I. A. M. E. Giebels, E. S. Kooij, N. J. Koeman, J. H. Rector, A. T. M. van Gogh, and R. Griessen (unpublished).
- <sup>27</sup>J.M. Boulet and N. Gerard, *J. Less-Common Met.* **89**, 151 (1983).
- <sup>28</sup>A. Pebler and W.E. Wallace, *J. Phys. Chem.* **66**, 148 (1962); C.E. Lundin and J.P. Blackledge, *J. Electrochem. Soc.* **109**, 838 (1962); H.E. Flotow, D.W. Osborne, K. Otto, and B.M. Abraham, *J. Chem. Phys.* **38**, 2620 (1962).
- <sup>29</sup>Although in Fig. 1 we display only the results for  $24^\circ \leq 2\theta \leq 36^\circ$ , the entire range ( $10^\circ \leq 2\theta \leq 75^\circ$ ) is used in our analysis.
- <sup>30</sup>As the volume per YMg formula unit is slightly (1.8%) smaller than the added volumes of pure Y and Mg (see Ref. 25), we make a small error (compared to the volume changes upon hydrogenation) by starting from the Y and Mg volumes.
- <sup>31</sup>F.H. Ellinger, C.R. Holley, Jr., B.B. McInnteer, D. Pavone, R.M. Potter, E. Starizky, and W.H. Zachariasen, *J. Am. Chem. Soc.* **77**, 2647 (1955); T. Schober, *Metall. Trans. A* **12A**, 951 (1981).
- <sup>32</sup>Note that for  $z=0.5$  we find evidence of the *orthorhombic*  $\gamma$ - $\text{MgH}_2$  structure, which is reported to exist at high pressures ( $\sim 80$  kbar) only. See J.-P. Bastide, B. Bonnetot, J.-M. Letoffe, and P. Claudy, *Mater. Res. Bull.* **15**, 1215 (1980); M. Bortz, B. Bertheville, G. Böttger, and K. Yvon, *J. Alloys Compd.* **287**, L4 (1999).
- <sup>33</sup>Recently, Wijngaarden *et al.* used a diamond anvil cell (DAC) to apply high pressures ( $\leq 25$  GPa) to  $\text{YH}_{3-\delta}$ . In contrast to our findings, they do not report a transition from hcp to fcc. It is not completely clear to us why the two experiments yield different conclusions. It might be due to the fact that the pressure medium in the DAC was liquid/solid  $\text{H}_2$ , whereas in our experiment we have gaseous  $\text{H}_2$  at a pressure of 1 bar. See R.J. Wijngaarden, J.N. Huiberts, D.G. Nagengast, J.H. Rector, R. Griessen, M. Hanfland, and F. Zontone, *J. Alloys Compd.* **308**, 44 (2000).
- <sup>34</sup>S.N. Sun, Y. Wang, and M.Y. Chou, *Phys. Rev. B* **49**, 6481 (1994).
- <sup>35</sup>A.T.M. van Gogh, E.S. Kooij, and R. Griessen, *Phys. Rev. Lett.* **85**, 2156 (2000); A. T. M. van Gogh, D. G. Nagengast, E. S. Kooij, N. J. Koeman, J. H. Rector, R. Griessen, C. F. J. Flipse,

- and R. J. J. G. A. M. Smeets, Phys. Rev. B **63**, 195105 (2001).
- <sup>36</sup>I. A. M. E. Giebels, J. Isidorsson, E. S. Kooij, A. Remhof, N. J. Koeman, J. H. Rector, A. T. M. van Gogh, and R. Griessen, J. Alloys Compd. (to be published).
- <sup>37</sup>When the optical properties change as a function of sample temperature (at constant  $p_{\text{H}_2}$  or cell volume) one speaks of thermochromism. In this case we consider the optical transmittance only. For more details, see Ref. 24.
- <sup>38</sup>S. J. van der Molen, W. H. Huisman, and R. Griessen, J. Alloys Compd. (to be published).
- <sup>39</sup>S. J. van der Molen, M. S. Welling, and R. Griessen, J. Alloys Compd. (to be published).
- <sup>40</sup>P. van Gelderen, P. J. Kelly, and G. Brocks, Phys. Rev. B **63**, 100301 (2001).
- <sup>41</sup>J.N. Huiberts, R. Griessen, R.J. Wijngaarden, and M. Kremers, Phys. Rev. Lett. **79**, 3724 (1997).
- <sup>42</sup>Hall measurements show that at room temperature  $\approx 0.2\%$  of the H vacancies donate an electron to the conduction band (see Ref. 41). At the rest of the vacancy sites, localized electrons are trapped, most likely in an *S*-like state (see Ref. 16).
- <sup>43</sup>S. Kirkpatrick, Rev. Mod. Phys. **45**, 574 (1973); D. Stauffer and A. Aharony, *Introduction to Percolation Theory*, 2nd ed. (Taylor and Francis, London, 1998).
- <sup>44</sup>J.R. Lacher, Proc. R. Soc. London, Ser. A **161**, 525 (1937).
- <sup>45</sup>L.E. Brus, J. Chem. Phys. **80**, 4403 (1984).
- <sup>46</sup>L.T. Canham, Appl. Phys. Lett. **57**, 1046 (1990); T. Takagahara and K. Takeda, Phys. Rev. B **46**, 15 578 (1992); J.P. Proot, C. Delerue, and G. Allan, Appl. Phys. Lett. **61**, 1948 (1992); G. Fishman, I. Mihalcescu, and R. Romestain, Phys. Rev. B **48**, 1464 (1993).